

Mechanism of activation of the *Drosophila* EGF Receptor by the TGF α ligand Gurken during oogenesis

Christian Ghiglione^{1,*}, Erika A. Bach¹, Yolande Paraiso*, Kermit L. Carraway III^{3,†}, Stéphane Noselli* and Norbert Perrimon^{1,2,§}

¹Department of Genetics, Medical Institute, Harvard Medical School, 200 Longwood Avenue, Boston, MA 02115, USA

²Howard Hughes Medical Institute, Harvard Medical School, 200 Longwood Avenue, Boston, MA 02115, USA

³Division of Signal Transduction, Beth Israel Deaconess Medical Center, 330 Brookline Avenue, Boston, MA 02215

*Present address: Centre de Biochimie. UMR6543/CNRS. Faculté des Sciences. 06108 Nice, France

†Present address: UC Davis Cancer Center, 4645 2nd Avenue, Sacramento, CA 95817, USA

§Author for correspondence (e-mail: perrimon@rascal.med.harvard.edu)

Accepted 4 October 2001

SUMMARY

We have analyzed the mechanism of activation of the Epidermal growth factor receptor (Egfr) by the transforming growth factor (TGF) α -like molecule, Gurken (Grk). Grk is expressed in the oocyte and activates the Egfr in the surrounding follicle cells during oogenesis. We show that expression of either a membrane bound form of Grk (mbGrk), or a secreted form of Grk (secGrk), in either the follicle cells or in the germline, activates the Egfr. In tissue culture cells, both forms can bind to the Egfr; however, only the soluble form can trigger Egfr signaling,

which is consistent with the observed cleavage of Grk in vivo. We find that the two transmembrane proteins Star and Brho potentiate the activity of mbGrk. These two proteins collaborate to promote an activating proteolytic cleavage and release of Grk. After cleavage, the extracellular domain of Grk is secreted from the oocyte to activate the Egfr in the follicular epithelium.

Key words: *gurken*, *Star*, *rhomboid-1*, *brother of rhomboid*, Oogenesis, *Drosophila*, Egfr

INTRODUCTION

The mammalian epidermal growth factor receptor (EGFR) is a member of the ErbB family of receptor tyrosine kinases (RTKs) that has been implicated in cellular proliferation, migration and differentiation, as well as the generation and progression of tumors (Moghal and Sternberg, 1999). Although there has been a great deal of progress towards understanding how signal transduction through these receptors is regulated, less is known about the mechanisms that control production of active forms of their ligands.

Like its vertebrate homologs, the *Drosophila* EGFR (Egfr) mediates various inductive signaling events in several tissues to regulate normal embryonic and adult development (Ray and Schüpbach, 1996; Perrimon and Perkins, 1997; Schweitzer and Shilo, 1997). The Egfr is involved in many different aspects of development and its signaling activity is precisely controlled by both activating and inhibiting ligands (Perrimon and McMahon, 1999; Freeman, 2000).

The multiple tissue-specific activities of the Egfr are regulated in part by three activating ligands: Vein (Vn) (Schnepp et al., 1996), Spitz (Spi) (Rutledge et al., 1992) and Gurken (Grk) (Neuman-Silberberg and Schüpbach, 1993). Each of these ligands contains an EGF repeat similar to that of transforming growth factor α (TGF α), a known ligand of the vertebrate EGFR. Vn is most similar to the mammalian

neuregulin ligand, which possesses an immunoglobulin (Ig)-like domain in addition to the core EGF domain. Vn has a spatially regulated expression pattern and is required for cell proliferation during embryogenesis and for cell fate determination in the embryo and wing (Schnepp et al., 1996; Simcox et al., 1996; Yarnitzky et al., 1997). As it is a soluble, secreted protein, it may not need processing for its activation.

Spi is required in many developmental processes (Schweitzer and Shilo, 1997; Wasserman and Freeman, 1998). Like the Egfr itself, *spi* expression is temporally and spatially broad, raising the question of how the precise activation of the Egfr is achieved. The mechanism that underlies this regulation relies in tightly controlled post-translational activation of Spi. Like its mammalian counterpart TGF α , Spi is expressed as a functionally inactive transmembrane protein with the active EGF domain outside the cell. Subsequent proteolytic cleavage of the extracellular portion of the molecule generates a soluble and potent Egfr ligand (Freeman, 1994; Schweitzer et al., 1995a; Golembo et al., 1996).

The activation of Spi requires two additional proteins (Schweitzer et al., 1995a; Guichard et al., 1999), Rhomboid-1 (Rho-1), a predicted seven transmembrane domains protein (Bier et al., 1990), and Star (S), a single-pass transmembrane protein (Kolodkin et al., 1994). Consistent with this view, *rho-1*, *S* and *spi* mutants have nearly identical embryonic phenotypes (Bier et al., 1990; Mayer and Nüsslein-Volhard,

1988; Rutledge et al., 1992). In contrast to *S*, *spi* and *Egfr*, which are expressed ubiquitously in most tissues, *rho-1* is expressed in a spatially restricted and dynamic pattern (Bier et al., 1990). Localized expression of *rho-1* correlates with cells having an elevated activity of Egfr activity, as revealed by high levels of MAPK activation detected in vivo (Gabay et al., 1997a; Gabay et al., 1997b; Guichard et al., 1999). These observations suggest that Rho-1 provides the spatial and temporal clues necessary for restricting Egfr activation to the appropriate cells during development. More recently, Bang and Kintner (Bang and Kintner, 2000) have used a heterologous assay system in *Xenopus* to demonstrate that the primary function of Rho-1 and *S* may not be to promote mbSpi cleavage, but rather to modify its presentation, which in some cases may also lead to ligand processing.

Grk encodes another TGF α -like ligand of the Egfr. Grk is expressed exclusively in the female germline (Neuman-Silberberg and Schüpbach, 1993), and regulates the activity of the Egfr which is expressed in the surrounding follicle cells (Price et al., 1989; Sapir et al., 1998). During *Drosophila* oogenesis, several intercellular communication events, involving the Grk/Egfr pathway, occur between the germline and the follicle cells (Nilson and Schüpbach, 1999). These cell-cell communication events are required to establish both the anteroposterior (AP) and the dorsoventral (DV) axes of the egg chamber, thus defining the polarity of both the egg and the future embryo (Morasito and Anderson, 1995; Ray and Schüpbach, 1996). During early oogenesis, Grk induces posterior follicle cell fates, thus establishing the AP axis. At later stages, when the oocyte has grown and the nucleus has moved to the anterior-dorsal corner of the oocyte, *grk* mRNA and protein become asymmetrically localized. Grk then activates the Egfr in overlying follicle cells and induces them to adopt a dorsal cell fate (Nilson and Schüpbach, 1999; Van Buskirk and Schüpbach, 1999). Properly patterned follicle cells then secrete a polarized eggshell and regulate the production of a new signal that establishes DV polarity in the embryo (Nilson and Schüpbach, 1999).

Despite the critical role of the Grk/Egfr pathway during oogenesis, little is known about the mechanism by which Grk activates the Egfr. For example, it is not known whether Grk is cleaved, as proposed for Spi, or whether it acts as a membrane-bound ligand. In this report, we show that overexpression of both mbGrk and secreted Grk in somatic tissues and in the oocyte can activate the Egfr pathway. However biochemical analyses reveal that whereas both forms of Grk can bind to the receptor, only the soluble form can activate the Egfr pathway. In addition, we show that Grk is cleaved in the oocyte and that *S* and *Brho*, a recently identified Rho-related protein (Guichard et al., 2000), collaborate to promote this processing. Altogether, our results reveal that Grk is activated by a mechanism similar to that for Spi.

MATERIALS AND METHODS

Fly stocks

The following Gal4 lines were used: CY2-Gal4 (Queenan et al., 1997), 55B-Gal4 (Brand and Perrimon, 1994), MS1096-Gal4 (Capdevila and Guerrero, 1994), nos-Gal4 and pCOG-Gal4 (Rorth, 1998). UAST-*mbSpi*, UAST-*S* and UAST-*rho-1* were a gift from A.

Michelson. UAST-*brho* and the *S* alleles (*S*²¹⁸ and *S*^l) were a gift from A. Guichard (Guichard et al., 2000). Deficiencies for *brho*: Df(3L)5411, Df(3L)5412, Df(3L)4214, Df(3L)2399 and Df(3L)57, were obtained from the Bloomington stock center.

*S*²¹⁸ mitotic clones in the follicle cells were generated using the *FRT40; T155-UASFLP* chromosome (Duffy et al., 1998). *S*²¹⁸ germline clones were generated as previously described (Chou and Perrimon, 1996). Wings and eggs were mounted in Hoyer's medium for microscopic examination.

Construction of plasmids and generation of transgenic lines

Cloning details for making these constructs are available by request. The coding regions of *rho-1* (Bier et al., 1990), *brho* (Guichard et al., 2000), *spi* (Rutledge et al., 1992), *secspi*, *S* (Kolodkin et al., 1994), *grk* (Neuman-Silberberg and Schüpbach, 1993), *secgrk*, *mbgrk*^{myc} and *mbgrk Δ 19AA*^{myc} were subcloned into the P-element vector pUAST (Brand and Perrimon, 1993) and/or pUASP (Rorth, 1998). *mbgrk*^{myc} and *mbgrk Δ 19AA*^{myc} were made by cloning six consecutive Myc tags at the C terminus. The coding regions of *S* and *brho* were subcloned in reverse orientation into pUASp to give antisense UASp. The UAS constructs were then introduced into flies by standard methods of P-element-mediated germline transformation of *w*¹¹¹⁸ embryos.

Insect cell experiments

Sf9 cell experiments

Recombinant baculoviruses encoding Egfr and Kek1 were described previously (Ghiglione et al., 1999). Baculovirus encoding AOS was from M. Freeman (Schweitzer et al., 1995b). For recombinant viruses encoding the mbGrk, secGrk, coding regions were subcloned into the insect cell expression vectors pVL1392 or pVL1393 (Invitrogen). Recombinant viruses were produced in Sf9 insect cells using the Bac-N-Blue transfection kit (Invitrogen) and were plaque purified before use.

For the aggregation experiments, populations of Sf9 cells in Grace's complete media were independently infected with wild-type baculovirus, or virus encoding Egfr, mbGrk, secGrk, AOS or Kek1 for 72 hours. Cells were harvested, pelleted and the conditioned media from wild-type, secGrk or AOS cells was saved. Cell pellets were resuspended at 2 \times 10⁶ cells/ml in fresh media or for blocking experiments cells were resuspended in conditioned media from wild-type, secGrk or AOS-expressing cells. Resuspended cells were mixed at a 1:1 ratio and incubated for 1 hour with gentle agitation. Cells were then examined for aggregation.

Egfr activation assay

S2:Egfr cells were maintained in culture as previously described (Schweitzer et al., 1995a). These cells stably express the metallothionein (Mt) *Egfr* plasmid, and Egfr expression is induced by addition of CuSO₄ to the cells (Schweitzer et al., 1995a). S2:Egfr cells (2 \times 10⁶) were incubated for 3 hours with 60 μ M CuSO₄ to induce moderate levels of Egfr expression. The cells were harvested by scraping and transferred into 1.5 ml microfuge tubes. The cells were stimulated in a total volume of 1 ml for 30 minutes with serum-free media (SFM), or with mbGrk, secGrk or secSpi, all made in baculovirus. Cells were pelleted by centrifugation and immediately lysed for 10 minutes at 4°C in lysis buffer (150 mM NaCl; 50 mM Tris pH 7.5; 1% Triton X-100; with inhibitors 1 mM PMSF, 1 mM EDTA, 1 mM EGTA, 5mM Iodoacetamide, 10 mg/ml aprotinin and leupeptin and 1mM NaOH). Lysates were fractionated by centrifugation at 10000 *g* for 10 minutes at 4°C. The supernatants were transferred to new 1.5 ml microfuge tubes. For immunoprecipitation of Egfr, 0.5 μ l of rabbit anti-Egfr (a kind gift from N. Baker) was added and the lysates were incubated on a rotary wheel at 4°C for 45 minutes. Washed Protein A-Sepharose (30 μ l) was then added to each lysates for 45 minutes at 4°C on a rotary wheel. The immunoprecipitates were washed with 3 \times 1 ml lysis buffer.

2× Laemmli buffer was then added and the precipitates heated at 70°C for 5 minutes. The precipitates were resolved by SDS-PAGE on a 6% gel under reducing conditions, and the gel was blotted onto Immobilon membrane. The membrane was blocked for 45 minutes in phosphate-buffered saline (PBS) with 0.5% Tween 20 and 3% bovine serum albumin (BSA). Egfr tyrosine phosphorylation was examined by Western blotting (at 1:5000) with mAb RC-20 (Transduction Laboratories). The blot was then stripped and reprobed with rabbit anti-Egfr polyclonal sera (a kind gift from M. Freeman), used at 1:1000, followed by HRP-Donkey anti-rabbit (Jackson ImmunoResearch Laboratories). Western blots were developed with enhanced chemiluminescence (ECL, Amersham).

Grk cleavage in S2 cells

S2 cells were transiently transfected with constructs under the control of Ac5c promoter using a calcium phosphate transfection kit following the manufacturer's instructions (Invitrogen). Seventy-two hours after transfection, the cells and their conditioned media were harvested by aspiration, collected and centrifuged at 1500 rpm for 7 minutes. The supernatants were transferred to new tubes and centrifuged again at 2000 rpm for 10 minutes to pellet any cells and cellular debris. Grk molecules in the conditioned media were immunoprecipitated by incubation with 30 µl of mouse anti-Grk and 50 µl of Protein G-Sepharose. The precipitates were washed 3×1 ml of ice-cold lysis buffer.

The transfected cells were lysed for 10 minutes in ice-cold lysis buffer. The lysates were centrifuged at 10000 g for 10 minutes at 4°C. The soluble fractions containing the cytosolic and plasma membrane components were transferred to new microfuge tubes.

Laemmli buffer (2×) was added to the lysates and to the immunoprecipitates. The samples were heated at 70°C for 5 minutes then resolved by SDS-PAGE on 10% gel under reducing conditions. Grk was immunoblotted by incubation using a 1:50 dilution of the anti-Grk antibody and detected using a HRP-conjugated anti-mouse antibody (1:10000) from Amersham. The western blots were developed with ECL. Immunoblotting for various proteins was performed as described above. S^{myc} was detected using a mouse anti-Myc monoclonal antibody 9E10 (Calbiochem, 1:500) or a rabbit anti-Myc polyclonal sera (Santa Cruz, 1:200); Brho^{GFP} was detected using a rabbit anti-GFP (Molecular Probes, 1:400); Rho-1 was detected using a rabbit anti-Rho-1 (a kind gift from B. Shilo, 1:1000). The mouse anti-Grk (1D12) monoclonal antibody was a kind gift from T. Schüpbach and was also obtained from the Developmental Studies Hybridoma Bank.

Intracellular S and Brho localization

Forty-eight hours after transfection, S2 cells were harvested, allowed to adhere for 30 minutes to Lab-Tek 8-well chambered coverglass slides (Nalge Nunc International, Naperville, IL) that were coated with Poly-L-Lysine (Sigma Diagnostics, St Louis, MO). The cells were then fixed for 10 minutes with 4% formaldehyde in PBS, and permeabilized for 15 minutes in 0.1% Triton X-100. Cells were blocked with PBT containing 3% BSA for 10 minutes and subsequently stained for 1 hour at room temperature with the following antibodies diluted in PBT/3% BSA: rabbit anti-Myc (Santa Cruz) (1:200); mouse anti-*Drosophila* Golgi (Calbiochem) (1:30); and mouse anti-Rat KDEL (ER) (Calbiochem) (1:30). The cells with the Golgi- and ER-specific antibodies were then stained for 1 hour at room temperature in PBT containing 3% BSA with a 1:200 dilution of biotinylated goat anti-mouse (Vector). The cells stained by Myc-specific antibody were then stained for 1 hour at room temperature in PBT/3% BSA with a 1:400 dilution of Cy5 donkey anti-Rabbit (Jackson). The cells with biotinylated goat anti-mouse were then stained for 1 hour at room temperature in PBT/3% BSA with a 1:400 dilution of FITC-avidin (Vector) for Star^{myc} samples or with a 1:500 dilution of streptavidin Alexa Fluor 660 conjugate (Molecular Probes) for Brho^{GFP} samples. The cell outline was detected using a 1:50

dilution of Alex Fluor 568 Phalloidin for Brho^{GFP} samples or Alex Fluor 488 Phalloidin for Star^{myc} samples (both from Molecular Probes), which stains F-actin, for 20 minutes at room temperature. The stained cells were visualized using a Leica confocal microscope.

Immunoblot analysis

For preparation of ovarian extracts, 10 ovaries were dissected in ice-cold PBS. The PBS was removed and replaced with loading buffer. Ovaries were homogenized using a pestle, then centrifuged briefly to pellet debris. An equivalent of two ovaries per lane was loaded on a 10% SDS-PAGE gel under reducing conditions. The mouse monoclonal anti-Myc antibody 9E10 (Ab-1, Calbiochem) was used at 1:1000 and the HRP-conjugated secondary antibody (Vector) at 1:2000. The bands were visualized using ECL (Amersham).

Antibody staining

The Grk monoclonal antibody, 1D12, was raised against amino acids 53-185 from the Grk extracellular domain. Fixation and staining protocols are described elsewhere (Queenan et al., 1999). The monoclonal mouse anti-Myc antibody (Ab-1, Calbiochem) was used at 1:500, followed by FITC anti-mouse (Vector) at 1:500. Then, ovaries were washed, counterstained with phalloidin TRITC (Sigma) and mounted in Citifluor. Confocal images were collected on a Leica TCS confocal microscope.

RESULTS

Overexpression of either *mbGrk* or *secGrk* in follicle cells can activate the Egfr

We noticed that Grk, like TGF α and Spi, possess a putative dibasic signal (R₂₄₀ and K₂₄₁) that resembles a potential cleavage site (Brachmann et al., 1989; Wong et al., 1989; Schweitzer et al., 1995a) between the EGF and the transmembrane (TM) domains. To determine whether the extracellular domain of Grk alone is able to activate the Egfr, we generated a secreted form of Grk (*secGrk*) by inserting a stop codon after the dibasic putative cleavage site (Fig. 1A). This mutation leads to the deletion of both the TM and cytoplasmic domains. After transient expression in S2 cells, significant amount of *secGrk* was detected in the tissue culture medium (see below). To test the activity of these different forms of Grk, we analyzed the effect of overexpressing them using the UAS/Gal4 system (Brand and Perrimon, 1993). Several transgenic fly lines for UAS-*wild-type Grk* (*mbGrk*) and UAS-*secGrk* were generated and crossed to various Gal4 lines.

Overexpression of UAS-*mbGrk* in the ovarian follicle cells, using the CY2-Gal4 driver, leads to a weak dorsalization of the eggshell, as shown by the thickened dorsal appendages (Fig. 1C), which are spread further apart than in the wild-type controls (Fig. 1B). Examination of the cuticles reveals that the resulting embryos are also dorsalized (Fig. 1F). When overexpressed in the wing disc, using the MS1096-Gal4, UAS-*mbGrk* induces ectopic wing veins (Fig. 1I) that resemble moderate *Egfr* gain-of-function phenotypes. Our results are in contrast to previous reports (Queenan et al., 1999; Guichard et al., 2000) and suggest that *mbGrk* is able to activate weakly the Egfr signaling pathway in somatic tissues.

In contrast to the weak activation observed with UAS-*mbGrk*, overexpression of UAS-*secGrk*, using the same Gal4 lines, causes very strong gain-of-function phenotypes similar to those obtained when UAS-*Atop*, a constitutively activated

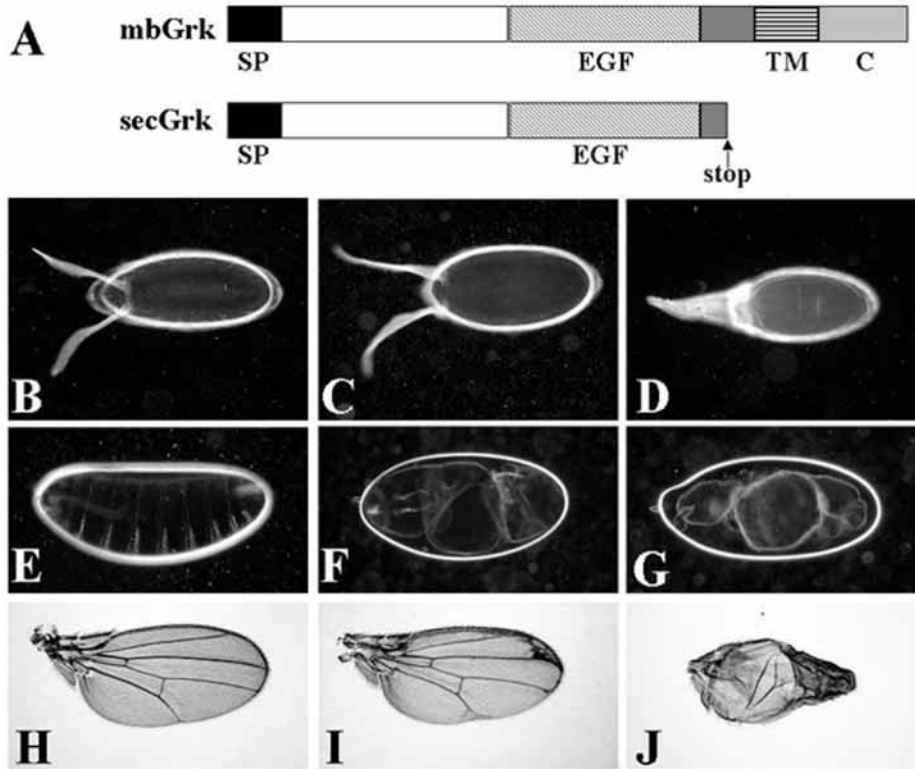


Fig. 1. *mbGrk* and *secGrk* overexpression in somatic tissues lead to *Egfr* activation. (A) Structure of *mbGrk* and *secGrk*. SP, signal peptide; EGF, EGF motif; TM, transmembrane domain; C, cytoplasmic domain. The arrow represents the site where the stop codon was introduced to generate *secGrk*. (B–J) Phenotypes observed after UAS-*mbGrk* and UAS-*secGrk* ectopic expression in somatic tissues. (B) Wild-type egg with its two dorsal appendages. (C) UAS-*mbGrk*/CY2: overexpression of *mbGrk* in all the follicular epithelium leads to a weak eggshell dorsalization (78% of the eggs, $n=352$). (D) UAS-*secGrk*/CY2: overexpression of *secGrk* leads to a very strong dorsalized eggshell phenotype (85% of the eggs, $n=244$). (E–G) Embryonic cuticles from: wild-type (E), UAS-*mbGrk*/CY2 (F) and UAS-*secGrk*/CY2 (G) females. (H) Wild-type wing with five longitudinal veins and two crossveins. (I, J) Weak and strong wing vein phenotypes associated with UAS-*mbGrk*/MS1096 (I) and UAS-*secGrk*/MS1096 wings (J).

Egfr, is misexpressed (Queenan et al., 1997). A strong dorsalization of the eggshell is clearly visible by the presence of a mass of dorsal appendage material around the entire anterior circumference of the egg (Queenan et al., 1999) (Fig. 1D). The cuticle of these embryos is also very strongly dorsalized (Fig. 1G). In addition, a very strong wing vein phenotype is observed after overexpression in the wing disc (Queenan et al., 1999) (Fig. 1J).

Altogether, these results indicate that *mbGrk* and *secGrk* are able to activate the *Egfr* when overexpressed in follicle cells. However, the strength of their activation differs: while *mbGrk* triggers weakly activation of *Egfr*, *secGrk* does it strongly. We also noticed a difference in the frequency of transgenic lines giving phenotypes: whereas all 12 UAS-*secGrk* lines trigger *Egfr* signaling, only two out of 20 UAS-*mbGrk* lines were associated with a weak dorsalization phenotype.

Overexpression of either *mbGrk* or *secGrk* in the germline can activate the *Egfr*

Next we tested the activity of the different Grk forms in the oocyte where Grk is normally expressed. However, because the original UAS/Gal4 system does not work in the female germline (Brand and Perrimon, 1993; Manseau et al., 1997), *mbGrk* and *secGrk* were subcloned into pUASp, a modified pUAST vector (Rorth, 1998). Subsequently, UASp-*mbGrk* and UASp-*secGrk* were overexpressed using the germline-specific Gal4 lines pCOG-Gal4 and/or nanos-Gal4 (nos-Gal4) (Rorth, 1998).

Overexpression of *mbGrk* and *secGrk* in the oocyte leads to activation of the *Egfr* pathway, as demonstrated by the dorsalization of the resulting eggs (Fig. 2A,B). In contrast to what we observed in somatic tissues, *mbGrk* gives a fully penetrant and stronger phenotype than *secGrk*. The frequency

of transgenic lines giving *Egfr* gain-of-function phenotypes is also reversed: whereas all the UASp-*mbGrk* lines strongly activate the *Egfr* pathway, only two out of 12 UASp-*secGrk* lines were associated with a weakly dorsalized phenotype. This is in contrast to a report by Queenan et al. (Queenan et al., 1999), who described that after expression in the oocyte using the endogenous *grk* promoter, *secGrk* was not able to activate the *Egfr*. This difference is probably due to a higher expression level of UASp-*secGrk*.

secGrk triggers *Egfr* autophosphorylation in vitro, but not *mbGrk*

Several membrane-bound ligands, such as proTGF α , CSF-1, proEGF and Kit ligand, need to be processed from a membrane-bound to a soluble form to activate their respective receptors; however, uncleaved membrane-bound ligands are also known to have signaling activity (Massague and Pandiella, 1993). Because both *mbGrk* and *secGrk* activate the *Egfr*, we performed tissue culture and biochemical experiments to determine the mechanism by which Grk activates the *Egfr*.

First, using an aggregation assay in Sf9 cells, we examined whether Grk binds to the *Egfr*. Cells expressing either *mbGrk* or the *Egfr* do not aggregate with themselves, or with cells infected with wild-type baculovirus (data not shown). However, when *mbGrk*-expressing cells are mixed with *Egfr*-expressing cells, these two kinds of cells strongly aggregate (Fig. 3A). *mbGrk* appears to bind selectively to the *Egfr* because there is no aggregation between *mbGrk*-expressing cells and cells expressing *Kek1*, a transmembrane protein that is able to bind and inhibit the *Egfr* (Ghiglione et al., 1999) (Fig. 3B). Furthermore, aggregation between *mbGrk* and *Egfr*-expressing cells could be fully and selectively blocked using conditioned media from cells expressing either *secGrk* (Fig.

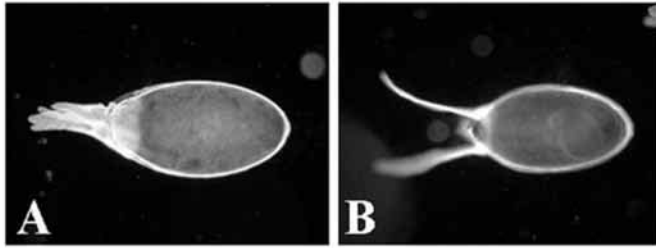


Fig. 2. UAS-*mbGrk* and UAS-*secGrk* overexpression in the oocyte leads to Egfr activation. (A) 100% ($n=122$) of the eggs derived from UASp-*mbGrk*/pCOG females exhibit a strong dorsalized eggshell. (B) Only 11% ($n=441$) of the eggs derived from UASp-*secGrk*/pCOG females exhibit a weak dorsalized eggshell.

3C) or Aos, a secreted Egfr inhibitor (Schweitzer et al., 1995b) (data not shown). These results indicate that mbGrk, expressed in one cell, is capable of interacting with the Egfr on an adjacent cell.

The initial event after activation of the EGFR is autophosphorylation of tyrosine residues on the C-terminal tail (Ullrich and Schlessinger, 1990). Biochemical analysis *in vitro* showed that Spi activates Egfr signaling: the addition of secreted Spi (secSpi), but not the membrane-associated form (mbSpi), to cultured cells expressing the Egfr is associated with a rapid autophosphorylation of Egfr on tyrosine residues (Schweitzer et al., 1995a). To test whether mbGrk and secGrk activate the Egfr, we used S2 cells stably transfected with the Egfr under the control of the metallothionein promoter. After induction with CuSO₄ (see Materials and Methods), a minimal level of spontaneous tyrosine phosphorylation was observed on the Egfr (data not shown), probably owing to overcrowding of Egfr molecules on the cell surface, which leads to spontaneous dimerization of receptor molecules (Schweitzer et al., 1995a). Addition of serum-free medium (SFM), or of

baculovirus-membranes expressing mbGrk to S2:Egfr cells, did not affect the level of phosphotyrosine residues on the Egfr. However, addition of baculovirus-generated secGrk or secSpi to the same cells results in a dramatic increase in the phosphotyrosine content of Egfr (Fig. 3D).

The tissue culture experiments described above confirm that Grk is a ligand of Egfr. Moreover, we have shown that mbGrk and secGrk can bind to the receptor, but only secGrk triggers Egfr autophosphorylation.

Grk is cleaved in the germline

As mbGrk does not activate the Egfr in tissue culture, we presumed that Grk must be cleaved to trigger Egfr signaling *in vivo*. To follow the cleavage of Grk *in vivo*, we generated a form of Grk that contains six Myc epitope tags at the C terminus (mbGrk^{myc}) (Fig. 4A). mbGrk^{myc} is fully active, as demonstrated by its ability to strongly dorsalize the egg after overexpression in the germline (Fig. 4B). The intracellular domain of Grk was then detected with an antibody against Myc, and compared with the overall distribution of Grk, which was detected using an antibody against the extracellular region (Peri et al., 1999; Queenan et al., 1999).

In the wild-type ovary, after expression of mbGrk^{myc} in the oocyte, the cytoplasmic portion of the mbGrk^{myc} protein remains confined to the oocyte (Fig. 4D). By contrast, the Grk antibody labels both in the oocyte and large dot-like structures in follicle cells. These structures presumably correspond to vesicular compartments, such as endosomes or lysosomes, that contain the extracellular domain of Grk (Peri et al., 1999; Queenan et al., 1999) (Fig. 4C).

Comparison of protein lysates from ovaries overexpressing mbGrk^{myc} in the oocyte and from wild-type, using an anti-Myc antibody, reveals the appearance of two bands in the lane corresponding to the protein lysates from ovaries overexpressing mbGrk^{myc} (Fig. 4E). The band around 70 kDa corresponds to the full-length mbGrk^{myc} protein, whereas the

Fig. 3. mbGrk and secGrk bind Egfr, but only secGrk triggers signaling. (A-C) Aggregation of mbGrk-expressing cells with Egfr cells. Sf9 insect cells were independently infected with wild-type baculovirus, or virus encoding Egfr, mbGrk or Kek1. The two populations of cells were mixed and incubated together for 1 hour and then examined. (A) Cells expressing mbGrk strongly aggregate to cells expressing Egfr. (B) Cells expressing mbGrk and cells expressing Kek1 do not aggregate. (C) Cells expressing mbGrk and cells expressing Egfr, in presence of conditioned medium from cells expressing secGrk, no longer aggregate. (D) secGrk but not mbGrk activates Egfr *in vitro*. S2:Egfr cells (2×10^6) were incubated for 3 hours with 60 μ M CuSO₄ to induce moderate levels of Egfr expression (Schweitzer et al., 1995a). The cells were then stimulated for 30 minutes with serum free media (SFM), mbGrk, secGrk or secSpi. Egfr precipitates were prepared using rabbit anti-Egfr polyclonal sera. Top: the level of tyrosine phosphorylation of the Egfr was assessed by western blotting with mAb RC-20 (PY). Bottom: Egfr expression was then assessed by western blotting with rabbit anti-Egfr polyclonal sera. The lower amounts of Egfr in secGrk and secSpi lanes are most probably due to incomplete stripping of the RC-20 antibody.

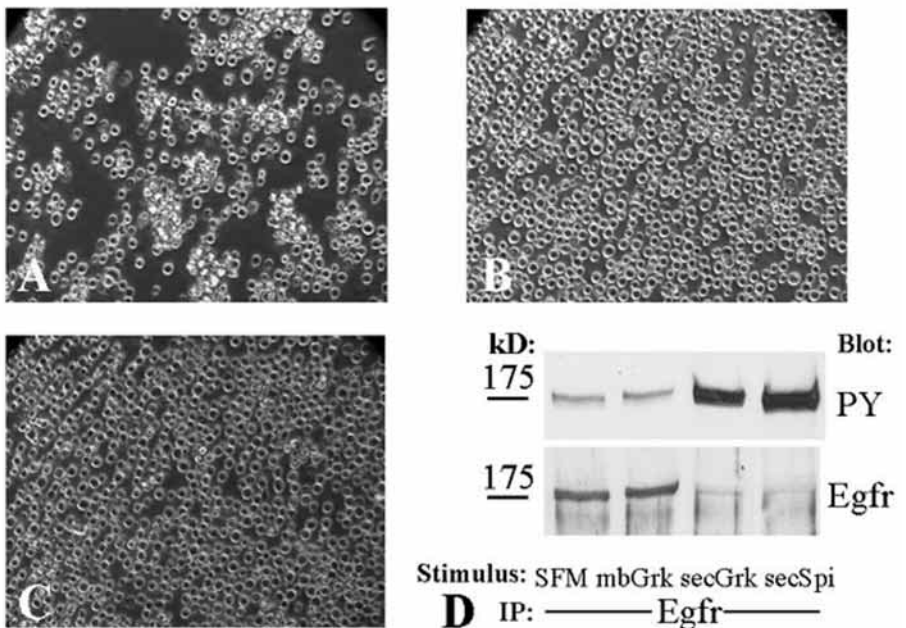
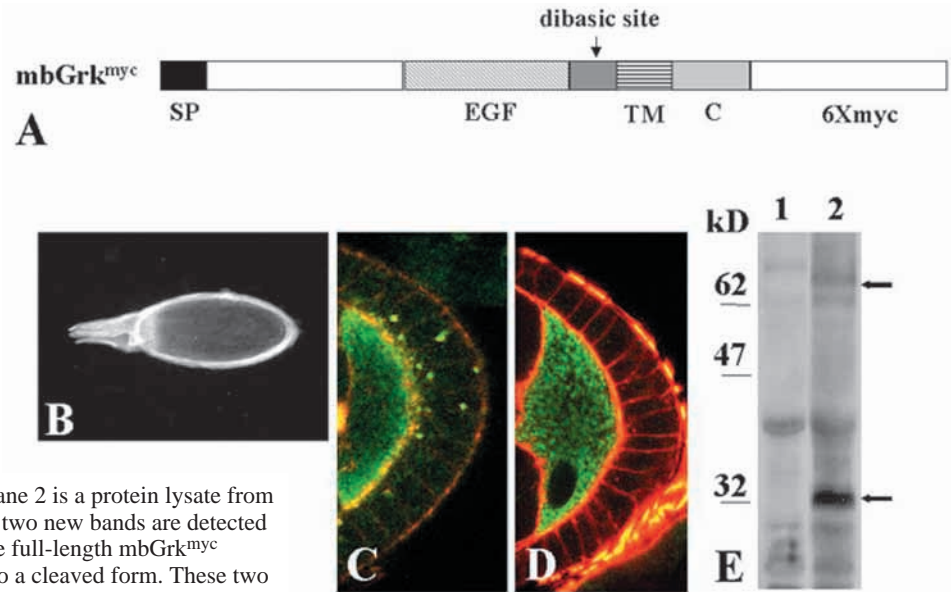


Fig. 4. The extracellular domain of Grk is released from the oocyte and internalized in follicle cells. (A) Structure of mbGrk^{myc}. (B) All eggs laid by UASp-*mbGrk^{myc}/nos-Gal4* females have a strongly dorsalized eggshell. (C,D) Confocal sections showing UASp-*mbGrk^{myc}/nos-Gal4* egg chambers stained with an anti-Grk antibody that detects the N-terminal region of the protein (C), or with an anti-Myc antibody that recognizes the intracellular region of the protein (D). While the uptake of the extracellular domain of Grk is clearly visible in follicle cells (C), the intracellular domain of Grk remains confined to the oocyte (D). Grk and Myc are in green, and actin is in red. (E) Western blot probed with anti-Myc antibody reveals a cleavage of mbGrk^{myc}. Lane 2 is a protein lysate from UASp-*mbGrk^{myc}/nos-Gal4* ovaries in which two new bands are detected (arrows). The higher band corresponds to the full-length mbGrk^{myc} protein whereas the lower one corresponds to a cleaved form. These two bands are absent in extracts from wild-type ovaries (lane 1).



band around 32 kDa corresponds to a cleaved form. Strikingly, the majority of the mbGrk^{myc} protein is cleaved, after overexpression in the oocyte, as shown by the relative small amount of the higher band compared with the lower one.

Altogether, these results indicate that Grk is cleaved in the oocyte. The Grk extracellular domain is taken up by follicle cells, while the intracellular domain remains confined to the oocyte.

Deletion of the region between the EGF and the TM domains creates a dominant-negative Grk protein

To determine whether mbGrk processing is required for Egfr activation, we mutated the putative dibasic cleavage signal (R₂₄₀ and K₂₄₁) of Grk. This mutation does not affect the ability of this mutant form of Grk to be cleaved and to activate the Egfr after overexpression in the oocyte (data not shown). Next, we deleted the sequence encoding 19 amino acids (Y₂₂₄ to V₂₄₂) located between the EGF and TM domains that contains the putative dibasic cleavage site (mbGrkΔ19AA^{myc}, Fig. 5A). When overexpressed in the oocyte, mbGrkΔ19AA^{myc} does not activate the Egfr. By contrast, the eggs laid by these females have fused dorsal appendages (Fig. 5B). The fusion of the dorsal appendages reflects a weak ventralization of the eggshell, a phenotype associated with *Egfr* or *grk* loss-of-function mutations (Schüpbach, 1987; Price et al., 1989). Western blot analysis of the protein lysates from ovaries expressing mbGrkΔ19AA^{myc} in the oocyte reveals that only the non-processed form of Grk^{myc} can be detected (Fig. 5C). The lower band described above, which corresponds to a processed form of Grk^{myc} (Fig. 4E), was never detected. The abolition of this cleavage also results in absence of uptake of the extracellular domain of this truncated protein in follicle cells (Fig. 5D). Finally, to test whether the absence of processing is the reason why mbGrkΔ19AA^{myc} is not associated with signaling activity, we generated another form of secGrk in which the stop codon was introduced immediately after the last amino acid (A₂₂₃) of the EGF domain. Overexpression of secGrk(A₂₂₃) in somatic tissues does not lead to any phenotype (data not shown).

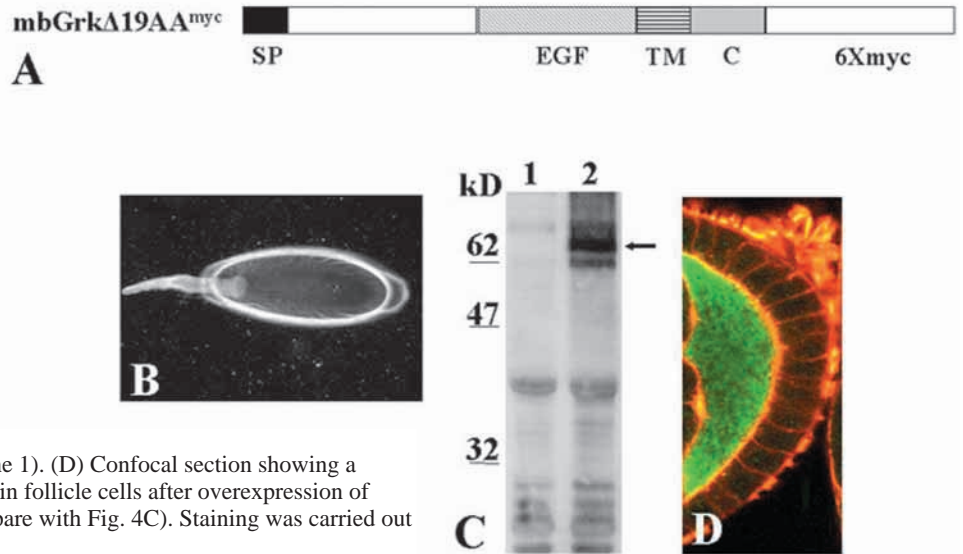
Altogether, our results indicate that the putative dibasic signal is not the cleavage site. However, we show that the 19 amino acid sequence located between the EGF and TM domains is important for Grk activity and cleavage. Overexpression of mbGrkΔ19AA^{myc} in the oocyte weakly ventralizes the eggshell, presumably by acting as a dominant-negative molecule.

Star and Brho are involved in the activation of Grk during oogenesis

Activation of the Egfr by the transmembrane ligand Spi, requires two transmembrane proteins, Rho-1 and Star (S). These proteins have been proposed to promote presentation and/or processing of mbSpi to generate an active diffusible form of the ligand (secSpi) (Schweitzer et al., 1995a; Pickup and Banerjee, 1999; Guichard et al., 1999; Bang and Kintner, 2000). Although S and Rho-1 act together at many developmental stages (Mayer and Nüsslein-Volhard, 1988; Schweitzer et al., 1995a; Guichard et al., 1999), this is not the case during oogenesis. Indeed S seems to be expressed exclusively in the germline (Pickup and Banerjee, 1999), whereas *rho-1* is expressed in the somatic follicle cells (Ruohola-Baker et al., 1993). However, a new *rho*-related gene called *brother of rhomboid* (*brho*) has been identified recently (Guichard et al., 2000). In contrast to *rho-1*, which is expressed in complex patterns during many stages of development (Bier et al., 1990; Ruohola-Baker et al., 1993), *brho* is expressed only in the early oocyte between stage 5 and 8 and in cells that abut the posterior follicle cells (Guichard et al., 2000). Thus, we were interested in examining the role of S and Rho family members in Grk activation.

As germline clones of S mutations do not develop beyond stage 1 of oogenesis (Nüsslein-Volhard et al., 1984) (this study, data not shown), and mutations in *brho* have not yet been identified (Guichard et al., 2000), we could not test directly the function of these two genes in the germline. Thus, we expressed antisense constructs of either UASp-*brho* or UASp-*S* in the germline. Interestingly, UASp-*S* antisense caused a

Fig. 5. Importance of the 19 amino acids located between the EGF and TM domains for Grk activity. (A) Structure of mbGrk Δ 19AA^{myc}. (B) 7% ($n=334$) of the eggs laid by UASp-mbGrk Δ 19AA^{myc}/nos-Gal4 females present a ventralized eggshell phenotype as shown by the fusion of the dorsal appendages. (C) Western blot probed with anti-Myc antibody reveals that, unlike mbGrk^{myc}, mbGrk Δ 19AA^{myc} is not cleaved when overexpressed in the oocyte (compare with Fig. 4E). Lane 2 is a protein lysate from UASp-mbGrk Δ 19AA^{myc}/nos-Gal4 ovaries. Only the higher band around 68 kDa that corresponds to the full-length mbGrk Δ 19AA^{myc}, is detected (arrow). This band is absent in wild-type ovaries (lane 1). (D) Confocal section showing a reduction of the uptake of extracellular Grk in follicle cells after overexpression of UASp-mbGrk Δ 19AA^{myc} in the oocyte (compare with Fig. 4C). Staining was carried out using an anti-Grk antibody.



ventralization of the eggshell, as shown by a complete fusion or disappearance of the dorsal appendages (Fig. 6A). In this assay, we did not obtain any significant phenotype after expressing a UASp-*brho* antisense construct (data not shown). To further examine the function of these genes in the germline, we overexpressed *S*, *rho-1* or *brho* using UASp, but did not detect any phenotypes. In addition, we were also unable to

detect any significant synergy after co-expressing mbGrk with each of these proteins, or after overexpressing mbGrk in flies heterozygous for either *S* or a deficiency of *brho* (data not shown).

To further examine the function of *S* and Rho-1/Brho in Grk activation, we turned to the follicle cell epithelium, where we have shown that ectopic expression of either mbGrk or secGrk is able to activate the Egfr (Fig. 1). Although Grk is not expressed in follicle cells, the presence of the Egfr and all the downstream components of the pathway allows us to test the synergy between Grk, *S* and Brho in this tissue. In follicle cells, there is a low level of *rho-1* (Ruohola-Baker et al., 1993) and no expression of *brho* (Guichard et al., 2000). Despite the recent evidence suggesting that *S* is not expressed in follicle cells (Pickup and Banerjee, 1999), we analyzed whether *S* is required for Egfr signaling in these cells. Interestingly, we found that *S* mutant follicle cell clones are associated with a weak ventralization of the eggshell, ranging from partially fused dorsal appendages to complete fusion (Fig. 6B). The phenotypes caused by loss of *S* in follicle cells resemble those caused by loss of *rho-1* (Ruohola-Baker et al., 1993; Wasserman and Freeman, 1998), and reflect the requirement of *S* and *rho-1* in the Spi-dependent activation of the Egfr.

To examine the relationship between *S* and Grk, we tested

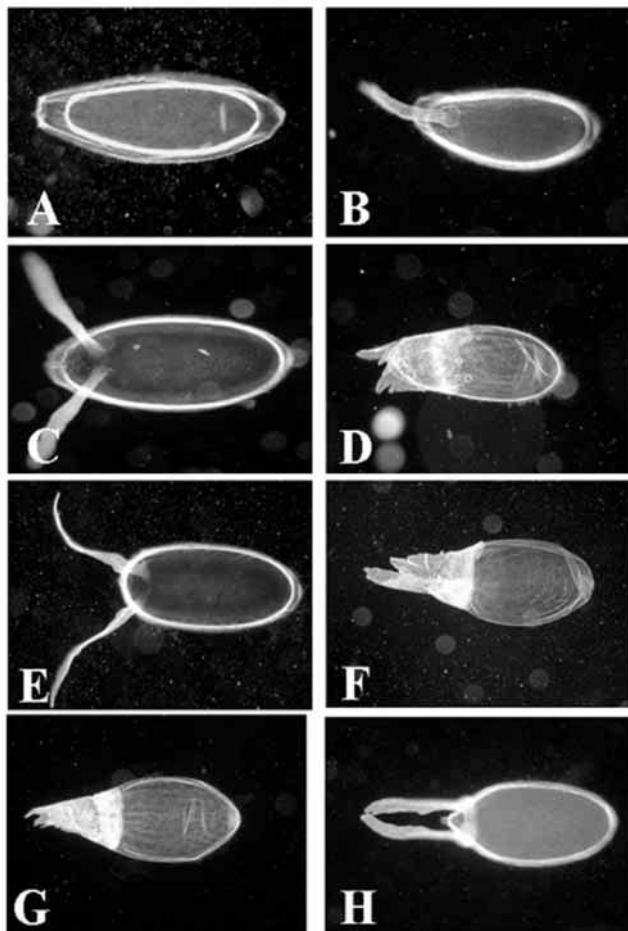
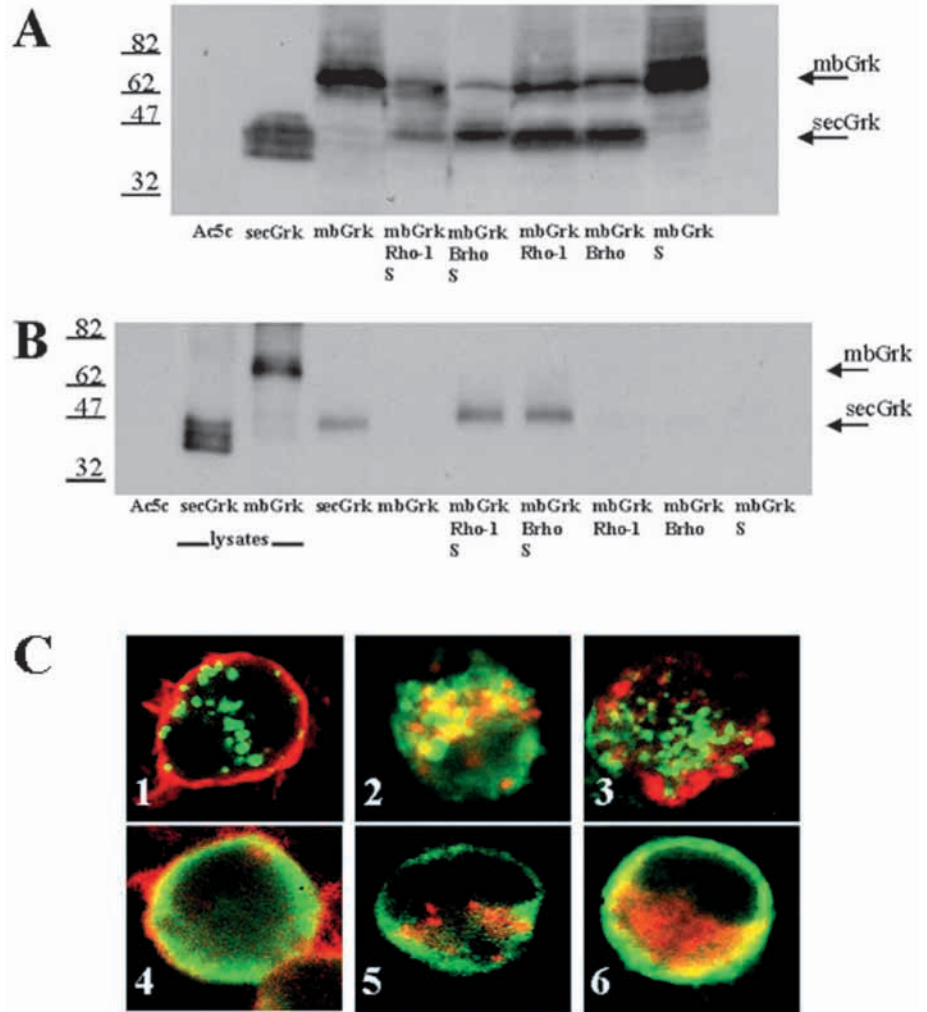


Fig. 6. Synergy between mbGrk, Star and Rho-related proteins during oogenesis. (A) Reduction of *S* by expressing an antisense UASp-*S* in the germline causes the ventralization of the eggshell (88%, $n=225$). (B) Dorsal appendages are fused in *S* mutant follicle cell clones. (C) Misexpression of UAS-mbGrk in *S*⁺ follicle cells results in a complete suppression of the mbGrk phenotype (compare with Fig. 1C). (D) Co-expression of UAS-*S* and UAS-mbGrk with CY2-Gal4 causes a strong eggshell dorsalization phenotype. (E) Ectopic expression of UAS-*brho* in the follicle cells using CY2-Gal4 causes a weak dorsalized eggshell phenotype. (F) Co-expression of UAS-mbGrk and UAS-*brho* in follicle cells induces a strong dorsalization of the eggshell. (G) Strong dorsalization of the eggshell after overexpression of mbSpi in the oocyte using pCOG-Gal4. (H) Ectopic expression of secSpi in the oocyte using the same driver causes a weaker dorsalized eggshell phenotype (33% of the eggs, $n=167$).

Fig. 7. S and Rho-1/Brho in S2 cells. S2 cells were transiently transfected with actin5c (Ac5c) driving expression of the indicated constructs. 72 hours after transfection, cellular lysates and conditioned media were analyzed by western blot with antibody raised against Grk extracellular domain. mbGrk^{myc} was used to distinguish easily the membrane-bound Grk and cleaved Grk forms. (A) Cell lysates: secGrk proteins exhibited M_r of about 40–45 kDa (lane 2), while mbGrk^{myc} displayed M_r around 70 kDa (lane 3). Lysates from S2 cells expressing mbGrk^{myc} with Rho-1 or Brho^{GFP} (lanes 6 and 7); or mbGrk^{myc} with Rho-1 or (Brho^{GFP}) and S^{myc} (lanes 4 and 5) contained both the mbGrk^{myc} form and also a cleaved form of Grk that migrated with the secGrk species (lane 2). Lysates from cells expressing mbGrk^{myc} with S^{myc} contained only the larger mbGrk^{myc} species and not the cleaved form of Grk (lane 8).

(B) Immunoprecipitates of conditioned media from the transfections described in A: no Grk was detected in media from cells expressing empty vector (lane 1), mbGrk^{myc} alone (lane 5), mbGrk^{myc} with Rho-1 or Brho^{GFP} (lanes 8 and 9, respectively), mbGrk^{myc} with S^{myc} (lane 10). The co-expression of mbGrk^{myc} with both S and Rho-1/Brho^{GFP} (lanes 6 and 7, respectively) leads to the accumulation of a soluble cleaved form of Grk in the medium that migrates with secGrk (lane 4). As control, secGrk and mbGrk^{myc} lysates were loaded on the same gel (lanes 2 and 3, respectively). We note that cleaved Grk released in the medium is slightly higher than the engineered secGrk. (C) S and Brho intracellular localization: S2 cells were transfected with Ac5c-Brho^{GFP} (C1–3) or Ac5c-S^{myc} (C4–6), both shown in green. The cells were also stained (all shown in red) with phalloidin to mark the plasma membrane (C1 and C4), anti-*Drosophila* Golgi mAb (C2 and C5) or anti-KDEL to mark the ER (C3 and C6). Brho is localized in discrete vesicles that colocalize with the Golgi apparatus (C2) and not the ER (C3). S is mostly expressed in a peri-plasma membrane pattern (C4). We note that some of S colocalizes with the ER (C6), however, none co-localizes with the Golgi (C5).



whether hyperactivation of the Egfr, after overexpression of UAS-*mbGrk* in follicle cells, requires S activity. We overexpressed UAS-*mbGrk*, using CY2-Gal4, in a S/+ heterozygous background. Reducing by half the dose of endogenous S leads to a complete suppression of the eggshell dorsalization phenotype (Fig. 6C; compare with Fig. 1C). A similar suppression was also observed in the wing (data not shown). Furthermore, we co-expressed S and mbGrk in follicle cells using CY2-Gal4. When this driver was used to overexpress S alone, no phenotype was observed (data not shown). However, co-expression of mbGrk and S caused a strong eggshell dorsalization phenotype (Fig. 6D), thus revealing a potent synergism between these two proteins, as has been previously seen in the wing (Guichard et al., 2000). These results indicate that, in the follicular epithelium, S can activate mbGrk.

In addition, we co-expressed mbGrk and Brho with CY2-Gal4 to test for synergy between these two proteins in the follicle cells. Whereas ectopic expression of UAS-*brho* causes only a weak dorsalized eggshell phenotype (Guichard et al.,

2000) (Fig. 6E), co-expression with UAS-*mbGrk* leads to a strong dorsalization phenotype (Fig. 6F), thus revealing an interaction similar to what has been previously reported in the wing (Guichard et al., 2000). We also observed similar synergy after co-expressing mbGrk and Rho-1 in the follicle cells (data not shown). Finally, co-expression of mbGrk with S and Brho using CY2-Gal4 leads to lethality (data not shown).

In light of our results obtained in the follicle cells and to explain our observations in the germline, we propose that the oocyte contains high levels of both S and Brho. Additional support for this model was obtained from misexpression experiments with Spi. First, unlike secSpi, mbSpi has been shown to be able to trigger Egfr activation following overexpression in somatic tissues only when simultaneously expressed with S and/or Rho-1 (Pickup and Banerjee, 1999; Guichard et al., 1999). Second, we observed a similar synergy between mbSpi, S and Rho-1/Brho in follicle cells (data not shown). Third, overexpression of UASp-*mbSpi* alone in the germline is associated with a strong dorsalized phenotype (Fig. 6G), and the average UASp-*secSpi* misexpression phenotype

is similar – although weaker – to the one induced by ectopic mbSpi in the oocyte (Fig. 6H).

Altogether, our results are consistent with the model that S and Brho, which are expressed highly in the germline, collaborate to activate mbGrk in the oocyte.

Grk cleavage in S2 cells

As S and Rho-1/Brho activate mbGrk when co-expressed in flies, we tested whether S and/or Rho-1/Brho are involved in Grk cleavage. To analyze this processing in detail, we used S2 cells that do not express either S or Rho-1/Brho (Schweitzer et al., 1995a; Guichard et al., 2000). S2 cells were transiently transfected with constructs encoding either secGrk or mbGrk, in absence or presence of S or Rho-1/Brho, or S and Rho-1/Brho. The mature Grk proteins of about 70 and 45 kDa could be detected in lysates from cells expressing mbGrk and secGrk, respectively (Fig. 7A). In addition, several secGrk intermediate forms ranging from 40 to 45 kDa, which probably represent glycosylation intermediates of the mature secGrk protein, were detected in cell extracts. Such intermediates have also been described for secSpi (Schweitzer et al., 1995a). Analysis of conditioned media from transfected cells reveals that mbGrk cannot be detected in the medium and that mbGrk is neither cleaved nor secreted in S2 cells. However, by contrast, significant amounts of only the mature form of secGrk can be detected in the conditioned medium (Fig. 7B).

Analysis of the conditioned media from different co-transfection experiments support the model that Rho-1/Brho are required for the cleavage of Grk and that the cleaved form of Grk is detected in the conditioned medium only when S is also present in these cells. First, lysates prepared from cells that co-expressed mbGrk with Rho-1/Brho or with Rho-1/Brho and S, contained both mbGrk and a cleaved form that migrates around the mature secGrk species. Second, only the mbGrk form can be detected in lysates from cells expressing mbGrk and S (Fig. 7A). Third, in cells expressing Rho-1/Brho and mbGrk, Grk is cleaved. However, in the absence of S, this cleaved Grk is not secreted in the medium (Fig. 7B).

To determine the subcellular localization of Brho and S, we transiently transfected S2 cells with constructs containing either Brho or S. We also stained these cells with phalloidin, to label filamentous actin and hence the plasma membrane, with an antibody specific for the *Drosophila* Golgi, and with a pan-ER antibody. Brho is expressed discretely in cytoplasmic vesicles (Fig. 7C1) that co-localize with the Golgi (Fig. 7C2) and not the ER (Fig. 7C3). S is expressed in a diffuse pattern in the cytoplasm, primarily in a peri-plasma membrane pattern (Fig. 7C4). Some of S colocalizes with the ER (Fig. 7C6) but none with the Golgi (Fig. 7C5).

Altogether, our results suggest that Rho-1/Brho are sufficient to catalyze Grk cleavage, and that S is involved in a trafficking/secretion process. The intracellular localization of S is also consistent with a role for S at a step that follows the Brho-dependent cleavage, as S is predominantly very close to the plasma membrane, while Brho localizes to the Golgi.

DISCUSSION

We have analyzed the mechanism of activation of the *Drosophila* Egfr by the TGF α homolog Grk. Grk is expressed

in the oocyte and activates the Egfr in the surrounding follicle cells. We demonstrate that the two transmembrane proteins Brho and S potentiate the activity of mbGrk. These two proteins collaborate to promote the proteolytic cleavage and secretion of the soluble extracellular domain of Grk. We present direct evidence supporting a proteolytic role for Rho-related proteins. Altogether, our results present the first direct evidence for Grk cleavage and have further provided insights into the function of both S and Rho proteins in this process.

Grk processing

Our in vivo and in vitro results clearly indicate that Grk is cleaved in the germline (see Fig. 4). An important question is where exactly the cleavage of the Grk precursor occurs? Bang and Kintner (Bang and Kintner, 2000) concluded that the cleavage of Spi occurs in the TM and depends on the 15 amino acid stretch located between the EGF and TM domains. Our results show that the Grk dibasic signal (R₂₄₀ and K₂₄₁) is not the cleavage site because its mutation does not abolish this event. However, mbGrk Δ 19AA^{myc}, in which the 19 amino acid (Y₂₂₄ to V₂₄₂) located between the EGF and TM domains have been deleted, is no longer cleaved, suggesting that this sequence is directly or indirectly involved in the processing.

Our results do not rule out the hypothesis that Grk cleavage occurs in the TM domain as proposed for Spi (Bang and Kintner, 2000). The high conservation between the Spi and Grk TM domains (Neuman-Silberberg and Schüpbach, 1993), in addition to aberrant Grk localization observed with different *grk* alleles affecting this TM domain (Queenan et al., 1999), reveal its importance. Moreover, the cleaved product of Grk that is released in the medium, after co-expressing mbGrk+S+Rho-1/Brho in S2 cells, has a slightly higher mobility than the engineered secGrk (Fig. 7B). Thus, it is possible that mbGrk is cleaved within the TM domain and that proteolysis depends on the 19 amino acid interval.

Our results reflect the importance of the Grk TM domain for proper processing and routing through the secretory pathway. mbGrk processing is probably tightly regulated and leads to efficient Grk secretion, contrary to engineered secGrk that is poorly secreted from the oocyte and that acts mainly intracellularly (Queenan et al., 1999) (this study).

Brho and S act in the germline to promote secretion of active Grk

The recent findings that S and Brho, a Rho-related protein, are expressed in the oocyte led us to investigate whether they are involved in Grk activation during oogenesis. S and Rho proteins have been proposed previously to be involved in the processing and activation of Spi (Klämbt, 2000); however, because they have no obvious motifs that predict their biochemical functions, their roles in ligand maturation and/or secretion has remained obscure.

The analysis of these proteins in the context of Grk signaling has provided numerous insights into the relationships between these transmembrane proteins. Our in vivo data strongly suggest that the expression level of S and Brho is very high in the oocyte, thus leading to an efficient cleavage and secretion of Grk. However, S and Rho-1 are probably expressed at low level in the follicle cells. Indeed, Pickup and Banerjee (Pickup and Banerjee, 1999) were unable to detect the presence of S in this epithelium using an anti-S antibody, whereas they clearly

showed a strong staining in the germline. The presence of both endogenous S and Rho-1 in follicle cells explains why overexpression of mbGrk in this epithelium leads to a weak dorsalization of the eggs. Nevertheless removing one copy of S is sufficient to completely suppress this phenotype. This confirms the observation that overexpression of mbGrk on its own is not able to activate the Egfr in vivo (Fig. 6C), as supported by our in vitro study (Fig. 3D). Overexpression experiments in follicle cells indicate a strong synergy between mbGrk, S, and Brho, as previously observed for Spi (Guichard et al., 1999; Guichard et al., 2000; Bang and Kintner, 2000) (Fig. 6). Further, co-expression of S and Rho-1/Brho is sufficient for Grk cleavage and secretion in S2 cells, strongly suggesting that they are the only proteins required for this process. In addition, these tissue culture experiments reveal that S and Rho-1/Brho are not obligate cofactors for this cleavage, because co-expression of mbGrk with Rho-1/Brho is sufficient to catalyze this proteolytic event (Fig. 7A). S is not required for Rho-1/Brho-mediated proteolytic cleavage in S2 cells, but the soluble Grk extracellular domain is no longer detected in the medium from these cells, indicating that the function of S is necessary for trafficking/secretion of the ligand. However, S is not able to cleave Grk in absence of Rho-1/Brho (Fig. 7A,B). Altogether, our results show that the functions of Rho-1/Brho and S are distinct, which explain their co-dependence and synergism in vivo (Guichard et al., 1999; Guichard et al., 2000).

How do Rho-1/Brho promote cleavage of mbGrk?

Rho-1/Brho may facilitate Grk proteolysis either by activating or recruiting a yet unknown protease. By analogy to the processing of mammalian Egfr ligands, Grk cleavage may be catalyzed by an ADAM-like metalloprotease (Black and White, 1998). Although these molecules are present in *Drosophila* (Wasserman et al., 2000), nothing is known yet about their functions. An alternative hypothesis, is that despite the absence of known protease domains in their sequences, Rho-1 and Brho themselves may have proteolytic activity. The subcellular localization of Brho, as observed for mature TACE (ADAM17) (Schlödorff et al., 2000), is predominantly in intracellular compartments (Fig. 7C1-3). In addition, and directly relevant to this hypothesis, Presenilins, which define another subfamily of seven-pass transmembrane proteins, have been proposed to encode proteases (Wolfe et al., 1999). In *Drosophila*, Presenilin may be directly responsible for the proteolysis of the intra-transmembrane domain of Notch (Struhl and Greenwald, 1999; Ye et al., 1999).

One of the striking feature of Rho-related proteins is that amino acid sequence conservation is most prominent in the predicted TM regions which contain some invariant charged residues (Guichard et al., 2000; Wasserman et al., 2000). This suggests the presence of a hydrophilic pocket that might constitute an enzymatic active site or a channel, as observed in Presenilins (Wolfe et al., 1999). This model is further supported by the recent finding that the TM domain of Spi is important for its functional interaction with Rho-1 (Bang and Kintner, 2000).

rho-related genes have been found in organisms from diverse kingdoms including *C. elegans*, rat, human, *Arabidopsis*, sugar cane, yeast and bacteria. Our data suggest that Brho, like Rho-1, promotes Egfr signaling by activating

TGF α -like ligands. As RTKs have not been found in plants (Satterlee and Sussman, 1998), yeast or bacteria, the *rho*-related genes in these organisms presumably serve other functions. It will be interesting to determine whether the activities of these Rho-related proteins are similar to those of Rho-1 and Brho, such as promoting the processing of proteins.

A possible role for S

Mosaic analysis of S, both in the germline (Nüsslein-Volhard et al., 1984) and in follicle cells (Fig. 6B), together with the S antisense experiment (Fig. 6A), demonstrate that S is required in follicle cells for Spi-dependent Egfr activation, and in the germline for Grk-dependent Egfr activation. Our tissue culture experiments suggest that S is not involved in Grk proteolysis, but instead in post-cleavage trafficking or secretion of the ligand (Fig. 7B). The intracellular localization of S is also consistent with a role for S at a step that follows the Brho-dependent cleavage, because we find that S is predominantly very close to, or at the plasma membrane (Fig. 7C4-C6), while Brho localizes to the Golgi (Fig. 7C2). The role of S, however, is not yet resolved because our results contrast with the ER localization of S in the oocyte described by Pickup and Banerjee (Pickup and Banerjee, 1999). Interestingly, unlike Rho-1 and Brho, S is probably involved in other processes as well. For example, S has been identified as a suppressor of Delta (Klein and Campos-Ortega, 1992), one of the Notch ligand. Delta encodes a transmembrane protein that is cleaved by the Kuzbanian metalloprotease, and the extracellular fragment antagonizes the function of the membrane-bound Delta protein as an activating Notch ligand (Klug et al., 1998; Qi et al., 1999). In the case of Notch signaling, a reduction of S gene activity might lead to a reduced release of the extracellular Delta fragment, and thus enhance Delta signaling (Klämbt, 2000).

Finally, understanding the function of S and Rho-1/Brho in Grk processing is relevant to studies of the mammalian ligands of the EGFR family as well, because TGF α may also be processed in vivo before receptor binding (Peschon et al., 1998). Thus, although further work is needed to fully understand the biochemical function of S, and Rho-1/Brho, our studies have provided a number of insights into the mechanism of action of these molecules.

We thank C. Arnold for generating the transgenic lines; A. J. Diamonti for expert technical assistance; N. Baker, A. Bang, M. Freeman, A. Guichard, A. Michelson, P. Rorth, B. Shilo and T. Schüpbach for reagents; and P. Léopold and P. Théron for sharing space and facility that allowed C. G. to complete this work. This work was supported by an EMBO fellowship (C. G.), The Jane Coffin Childs Memorial Fund for Medical Research (E. A. B.), NIH grant CA71702 (K. C.) the US Army Breast Cancer (N. P.) and la Ligue and l'ARC (C. G.). N. P. is an Investigator of the Howard Hughes Medical Institute.

REFERENCES

- Bang, A. G. and Kintner, C. (2000). Rhomboid and Star facilitate presentation and processing of the *Drosophila* TGF- α homolog Spitz. *Genes Dev.* **14**, 177-186.
- Bier, E., Jan, L. Y. and Jan, Y. N. (1990). *rhomboid*, a gene required for dorsoventral axis establishment and peripheral nervous system development in *Drosophila melanogaster*. *Genes Dev.* **4**, 190-203.

- Black, R. A. and White, J. M.** (1998). ADAMs: focus of the protease domain. *Curr. Opin. Cell Biol.* **10**, 654-659.
- Brachmann, R., Lindquist, M., Nagashima, M., Kohr, W., Lipari, T., Napier, M. and Derynck, R.** (1989). Transmembrane TGF- α precursors activate EGF/TGF- α receptors. *Cell* **56**, 691-700.
- Brand, A. H. and Perrimon, N.** (1993). Targeted expression as a means of altering cell fates and generating dominant phenotypes. *Development* **118**, 401-415.
- Brand, A. H. and Perrimon, N.** (1994). Raf acts downstream of the EGF receptor to determine dorsoventral polarity during *Drosophila* oogenesis. *Genes Dev.* **8**, 629-639.
- Capdevila, J. and Guerrero, I.** (1994). Targeted expression of the signaling molecule decapentaplegic induces pattern duplications and growth alterations in *Drosophila* wings. *EMBO J.* **13**, 4459-4468.
- Chou, T. B. and Perrimon, N.** (1996). The autosomal FLP-DFS technique for generating germline mosaics in *Drosophila melanogaster*. *Genetics* **144**, 1673-1679.
- Duffy, J. B., Harrison, D. A. and Perrimon, N.** (1998). Identifying loci required for follicular patterning using directed mosaics. *Development* **125**, 2263-2271.
- Freeman, M.** (1994). The spitz gene is required for photoreceptor determination in the *Drosophila* eye where it interacts with the EGF receptor. *Mech. Dev.* **48**, 25-33.
- Freeman, M.** (2000). Feedback control of intercellular signalling in development. *Nature* **408**, 313-319.
- Gabay, L., Seger, R. and Shilo, B. Z.** (1997a). In situ activation pattern of *Drosophila* EGF receptor pathway during development. *Science* **277**, 1103-1106.
- Gabay, L., Seger, R. and Shilo, B. Z.** (1997b). MAP kinase in situ activation atlas during *Drosophila* embryogenesis. *Development* **124**, 3535-3541.
- Ghiglione, C., Carraway, K. L., III, Amundadottir, L. T., Boswell, R. E., Perrimon, N. and Duffy, J. B.** (1999). The transmembrane molecule Kekk1 acts in a feedback loop to negatively regulate the activity of the *Drosophila* EGF receptor during oogenesis. *Cell* **96**, 847-856.
- Golembo, M., Raz, E. and Shilo, B. Z.** (1996). The *Drosophila* embryonic midline is the site of Spitz processing, and induces activation of the EGF receptor in the ventral ectoderm. *Development* **122**, 3363-3370.
- Guichard, A., Biehs, B., Sturtevant, M., Wickline, L., Chacko, J., Howard, K. and Bier, E.** (1999). *rhomboid* and *Star* interact synergistically to promote EGFR/MAPK signaling during *Drosophila* wing vein development. *Development* **126**, 2663-2676.
- Guichard, A., Roark, M., Ronshaugen, M. and Bier, E.** (2000). *Brother-of-rhomboid*, a *rhomboid*-related gene expressed during early *Drosophila* oogenesis, promotes EGF-R/MAPK signaling. *Dev. Biol.* **226**, 255-266.
- Klämbt, C.** (2000). EGF receptor signalling: the importance of presentation. *Curr. Biol.* **10**, R388-391.
- Klein, T. and Campos-Ortega, J. A.** (1992). Second-site modifiers of the *Delta* wing phenotype in *Drosophila melanogaster*. *Roux's Arch. Dev. Biol.* **202**, 49-60.
- Klug, K. M., Parody, T. R. and Muskavitch, M. A.** (1998). Complex proteolytic processing acts on *Delta*, a transmembrane ligand for Notch, during *Drosophila* development. *Mol. Biol. Cell.* **9**, 1709-1723.
- Kolodkin, A. L., Pickup, A. T., Lin, D. M., Goodman, C. S. and Banerjee, U.** (1994). Characterization of *Star* and its interactions with *sevenless* and EGF receptor during photoreceptor cell development in *Drosophila*. *Development* **120**, 1731-1745.
- Manseau, L., Baradaran, A., Brower, D., Elefant, F., Phan, H., Philp, A., Yang, M., Glover, D., Kaiser, K., Patler, K. and Selleck, S.** (1997). Gal4 enhancer traps expressed in the embryo, larval brain, imaginal discs, and ovary of *Drosophila*. *Dev. Dyn.* **209**, 310-332.
- Massague, J. and Pandiella, A.** (1993). Membrane-anchored growth factors. *Annu. Rev. Biochem.* **62**, 515-541.
- Mayer, U. and Nüsslein-Volhard, C.** (1988). A group of genes required for pattern formation in the ventral ectoderm of the *Drosophila* embryo. *Genes Dev.* **2**, 1496-1511.
- Moghal, N. and Sternberg, P.** (1999). Multiple positive and negative regulators of signaling by the EGF-receptor. *Curr. Opin. Cell Biol.* **11**, 190-196.
- Morisato, D. and Anderson, K. V.** (1995). Signaling pathways that establish the dorsal-ventral pattern of the *Drosophila* embryo. *Annu. Rev. Genet.* **29**, 371-399.
- Neuman-Silberberg, F. S. and Schüpbach, T.** (1993). The *Drosophila* dorsoventral patterning gene *gurken* produces a dorsally localized RNA and encodes a TGF α -like protein. *Cell* **75**, 165-174.
- Nilson, L. A. and Schüpbach, T.** (1999). EGF receptor signaling in *Drosophila* oogenesis. *Curr. Top. Dev. Biol.* **44**, 203-243.
- Nüsslein-Volhard, C., Wieschaus, E. and Kluding, H.** (1984). Mutations affecting the pattern of the larval cuticle in *Drosophila melanogaster*. I. Zygotic loci on the second chromosome. *Roux's Arch. Dev. Biol.* **193**, 267-282.
- Peri, F., Bökel, C. and Roth, S.** (1999). Local Gurken signaling and dynamic MAPK activation during *Drosophila* oogenesis. *Mech. Dev.* **81**, 75-88.
- Perrimon, N. and McMahon, A. P.** (1999). Negative feedback mechanisms and their roles during pattern formation. *Cell* **97**, 13-16.
- Perrimon, N. and Perkins, L. A.** (1997). There must be 50 ways to rule the signal: the case of the *Drosophila* EGF receptor. *Cell* **89**, 13-16.
- Peschon, J. J., Slack, J. L., Reddy, P., Stocking, K. L., Sunnarborg, S. W., Lee, D. C., Russell, W. E., Castner, B. J., Johnson, R. S. et al.** (1998). An essential role for ectodomain shedding in mammalian development. *Science* **6**, 1503-1517.
- Pickup, A. and Banerjee, U.** (1999). The role of *Star* in the production of an activated ligand for the EGF receptor signaling pathway. *Dev. Biol.* **205**, 254-259.
- Price, J. V., Clifford, R. J. and Schüpbach, T.** (1989). The maternal ventralizing locus *torpedo* is allelic to faint little ball, an embryonic lethal, and encodes the *Drosophila* EGF receptor homolog. *Cell* **56**, 1085-1092.
- Qi, H., Rand, M. D., Wu, X., Sestan, N., Wang, W., Rakic, P., Xu, T. and Artavanis-Tsakonas, S.** (1999). Processing of the Notch ligand *Delta* by the metalloprotease Kuzbanian. *Science* **283**, 91-94.
- Queenan, A. M., Ghabrial, A. and Schüpbach, T.** (1997). Ectopic activation of *Torpedo/Egfr*, a *Drosophila* receptor tyrosine kinase, dorsalizes both the eggshell and the embryo. *Development* **124**, 3871-3880.
- Queenan, A. M., Barcelo, G., Van Buskirk, C. and Schüpbach, T.** (1999). The transmembrane region of Gurken is not required for biological activity, but is necessary for transport to the oocyte membrane in *Drosophila*. *Mech. Dev.* **89**, 35-42.
- Ray, R. P. and Schüpbach, T.** (1996). Intercellular signaling and the polarization of body axes during *Drosophila* oogenesis. *Genes Dev.* **10**, 1711-1723.
- Rorth, P.** (1998). Gal4 in the *Drosophila* female germline. *Mech. Dev.* **78**, 113-118.
- Ruohola-Baker, H., Grell, E., Chou, T. B., Baker, D., Jan, L. Y. and Jan, Y. N.** (1993). Spatially localized rhomboid is required for establishment of the dorsal-ventral axis in *Drosophila* oogenesis. *Cell* **73**, 953-965.
- Rutledge, B. J., Zhang, K., Bier, E., Jan, Y. N. and Perrimon, N.** (1992). The *Drosophila* spitz gene encodes a putative EGF-like growth factor involved in dorsal-ventral axis formation and neurogenesis. *Genes Dev.* **6**, 1503-1517.
- Sapir, A., Schweitzer, R. and Shilo, B. Z.** (1998). Sequential activation of the EGF receptor pathway during *Drosophila* oogenesis establishes the dorsoventral axis. *Development* **125**, 191-200.
- Satterlee, J. S. and Sussman, M. R.** (1998). Unusual membrane-associated protein kinases in higher plants. *J. Membr. Biol.* **164**, 205-213.
- Schlöndorff, J., Becherer, J. D. and Blobel, C. P.** (2000). Intracellular maturation and localization of the tumour necrosis factor α convertase (TACE). *Biochem. J.* **347**, 131-138.
- Schnepf, B., Grumblin, G., Donaldson, T. and Simcox, A.** (1996). Vein is a novel component in the *Drosophila* epidermal growth factor receptor pathway with similarity to the neuregulins. *Genes Dev.* **10**, 2302-2313.
- Schüpbach, T.** (1987). Germline and soma cooperate during oogenesis to establish the dorsoventral pattern of the eggshell and embryo in *Drosophila melanogaster*. *Cell* **49**, 699-707.
- Schweitzer, R., Shaharabany, M., Seger, R. and Shilo, B. Z.** (1995a). Secreted Spitz triggers the DER signaling pathway and is a limiting component in embryonic ventral ectoderm determination. *Genes Dev.* **9**, 1518-1529.
- Schweitzer, R., Howes, R., Smith, R., Shilo, B. Z. and Freeman, M.** (1995b). Inhibition of *Drosophila* EGF receptor activation by the secreted protein Argos. *Nature* **376**, 699-702.
- Schweitzer, R. and Shilo, B. Z.** (1997). A thousand and one roles for the *Drosophila* EGF receptor. *Trends Genet.* **13**, 191-196.
- Simcox, A., Grumblin, G., Schnepf, B., Bennington, M. C., Hersperger, E. and Shearn, A.** (1996). Molecular, phenotypic, and expression analysis of *vein*, a gene required for growth of the *Drosophila* wing disc. *Dev. Biol.* **177**, 475-489.
- Struhl, G. and Greenwald, I.** (1999). Presenilin is required for activity and nuclear access of Notch in *Drosophila*. *Nature* **398**, 522-525.

- Ullrich, A. and Schlessinger, J.** (1990). Signal transduction by receptors with tyrosine kinase activity. *Cell* **61**, 203-212.
- Van Buskirk, C. and Schüpbach, T.** (1999). Versatility in signaling: multiple responses to EGF receptor activation during *Drosophila* oogenesis. *Trends Cell Biol.* **9**, 1-4.
- Wasserman, J. and Freeman, M.** (1998). An autoregulatory cascade of EGF receptor signaling patterns the *Drosophila* egg. *Cell* **95**, 355-364.
- Wasserman, J. D., Urban, S. and Freeman, M.** (2000). A family of rhomboid-like genes: *Drosophila rhomboid-1* and *roughoid/rhomboid-3* cooperate to activate EGF receptor signaling. *Genes Dev.* **14**, 1651-1663.
- Wolfe, M. S., Xia, W., Ostaszewski, B. L., Diehl, T. S., Kimberly, W. T. and Selkoe, D. J.** (1999). Two transmembrane aspartates in presenilin-1 required for presenilin endoproteolysis and γ -secretase activity. *Nature* **398**, 513-517.
- Wong, S. T., Winchell, L. F., McCune, B. K., Earp, H. S., Teixido, J., Massague, J., Herman, B. and Lee, D. C.** (1989). The TGF- α precursor expressed on the cell surface binds to the EGF receptor on adjacent cells, leading to signal transduction. *Cell* **56**, 495-506.
- Yarnitzky, T., Min, L. and Volk, T.** (1997). The neuregulin homolog Vein mediates inductive interactions between myotubes and their epidermal attachment cells. *Genes Dev.* **11**, 2691-2700.
- Ye, Y., Lukinova, N. and Fortini, M. E.** (1999). Neurogenic phenotypes and altered Notch processing in *Drosophila presenilin* mutants. *Nature* **398**, 525-529.